arXiv:2305.04777v2 [physics.optics] 9 May 2023

,

Reducing system dimensionality with long-range collective dipole-dipole interactions

Ashwin K. Boddeti,[1,2] Yi Wang,[3] Xitlali G. Juarez,[4] Alexandra Boltasseva,[1,2] Teri W. Odom,[3,4,5] Vladimir Shalaev,[1,2] Hadiseh Alaeian,[1,2,6] and Zubin Jacob[1,2,*]

[1] *Elmore Family School of Electrical and Computer Engineering, Purdue University, West Lafayette, Indiana 47907, USA*
[2] *Birck Nanotechnology Center, Purdue University, West Lafayette, Indiana 47907, USA*
[3] *Graduate Program in Applied Physics, Northwestern University, Evanston, IL, 60208 USA*
[4] *Department of Materials Science and Engineering, Northwestern University, Evanston, Illinois 60208, USA*
[5] *Department of Chemistry, Northwestern University, Evanston, Illinois 60208, USA*
[6] *School of Physics and Astronomy, Purdue University, West Lafayette, Indiana 47907, USA*

(Dated: May 10, 2023)

Dimensionality plays a crucial role in long-range dipole-dipole interactions (DDIs). We demonstrate that a resonant nanophotonic structure modifies the apparent dimensionality in an interacting ensemble of emitters, as revealed by population decay dynamics. Our measurements on a dense ensemble of interacting quantum emitters in a resonant nanophotonic structure with long-range DDIs reveal an effective dimensionality reduction to $\bar{d} = 2.20(12)$, despite the emitters being distributed in 3D. This contrasts the homogeneous environment, where the apparent dimension is $\bar{d} = 3.00$. Our work presents a promising avenue to manipulate dimensionality in an ensemble of interacting emitters.

Introduction- In a dense ensemble of interacting emitters, each emitter perceives the other neighboring emitters via position-dependent dipole-dipole interactions (DDIs). The role of geometry in such position-dependent collective interactions between an ensemble of emitters has been of fundamental interest [1–7]. Controlling the dimensionality is appealing as a lower-dimensional emitter geometry shows strong quantum fluctuations [8]. This can potentially provide a host of benefits in realizing platforms to probe long-range interactions [1, 2], quantum phases such as quantum spin-liquids [3, 4], transient super solid behavior [5], quantum phase transition in transverse Ising models [9], provide an advantage in quantum sensing applications, in mitigating decoherence [1, 5], and in long-range energy transport of delocalized excitons [7]. More recently, interesting physical effects on Dicke superradiance in 1D, 2D, and 3D arrays of atoms have been theoretically predicted [6]. Thus, realizing a lower-dimensional system supporting long-range DDIs is of significant importance.

While 1D and 2D interacting ensembles of emitters have been realized in cold-atom systems, it remains largely unexplored in solid-state platforms. Only recent efforts demonstrating a thin layer of emitters (NV - P1 centers) have paved the way for realizing lower-dimensional systems in solid states [1, 2]. The P1 system's many-body noise is characterized by the decoherence of NV center probe spins and shows stretched exponential decay dynamics [1].

As DDIs are mediated by the underlying electromagnetic fields, tailoring them provides an alternative route to manipulate the apparent dimensionality. Recently, interfacing quantum emitters with light within nanophotonic structures has provided the means to control and study collective DDIs [10]. This led to the demonstration of long-range resonance energy transfer in incoherent systems [11, 12], and sub-and super-radiant emission dynamics in coherent systems [13–16].

Here we modify the apparent dimensionality using a nanophotonic structure that supports dispersive delocalized resonant modes that mediate the interactions. These modes lead to modification of the spatial distribution of the perceived neighboring emitters. We experimentally probe the apparent dimensionality of the interacting ensemble of donor and acceptor emitters, encoded in the interacting emitters' temporal decay dynamics. While individual emitters decay exponentially, the lifetime decay dynamics of interacting ensemble of emitters follow a stretched exponential decay, revealing a non-integer power β in time,

$$I(t)/I_0 = exp(-\gamma_D t) exp(-\alpha t^{\beta}) \tag{1}$$

where γ_D is the spontaneous decay rate and α is the effective interaction volume [17–19]. The non-integer power, β, originates due to DDIs between the emitters and captures the apparent dimensionality sensed by the mutually interacting emitters.

$$\beta = \bar{d}/S \tag{2}$$

$\bar{d}$ is the apparent or fractal dimension, and $S = 6$ for electric DDIs [18]. Such relaxation decay dynamics arising due to DDIs are common in other systems such as the kinetic Ising model below the critical temperature, an interacting ensemble of spins [1], in ultra-cold atoms, and ions [20–25]. The underlying physics that governs

* zjacob@purdue.edu
www.electrodynamics.org

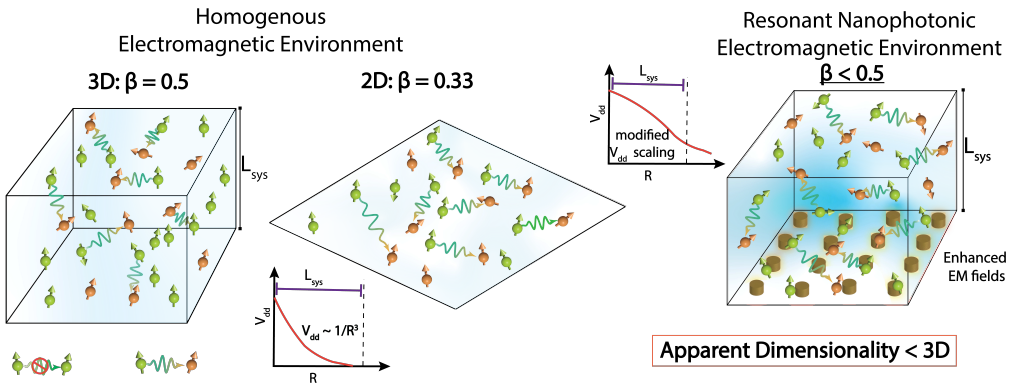

FIG. 1. The illustration depicts the concept of apparent dimensionality of an interacting ensemble of emitters. The apparent dimensionality is related to the non-integer exponent of time in the fluorescence decay dynamics $I(t)/I_0 = exp(-\gamma_D t)exp(-\alpha t^{\beta})$. In a homogeneous environment, $\beta = 0.5(0.33)$ for the 3D (2D) spatial distribution of emitters. A resonant nanophotonic environment modifies the spatial distribution of the neighboring emitters sensed by each interacting emitter which results in the modification of the temporal decay dynamics. This reduces the apparent dimensionality experienced by the interacting emitters, which is reflected in the non-integer exponent, $\beta < 0.5$, though, the emitters are distributed in a 3D volume.

DDIs is universal; here, we focus on DDIs at room temperature, where it is difficult to discern coherent effects.

The two underlying characteristics that relate to this intriguing non-integer power, β in the decay dynamics (and thus the apparent dimensionality) are (i) the distance scaling law associated with DDIs in the vicinity of nanophotonic environment and (ii) the competition between the characteristic DDI length-scale, R_0, and the system size, L_{sys}. The interplay between these two characteristic lengths determines the spatial extent of the emitters sensed by each donor quantum emitter. Figure 1 conceptually shows the origin of the reduced apparent dimensionality. In homogeneous environments, the DDI potential, V_{dd}, scales as $\sim 1/R^3$. The non-integer power, $\beta = 1/2$ (1/3) for the three-dimensional (two-dimensional) spatial distribution of emitters (see supplementary information) [17, 19, 26] for time-scales beyond the coherence times of the interacting system (i.e., the emitters do not possess memory of previous interaction events).

In contrast to homogeneous environments, a resonant nanophotonic structure modifies the strength, range, and characteristic interaction length scale of DDIs [11, 12, 14, 27, 28]. Due to this modification of underlying electromagnetic fields, an ensemble of interacting quantum emitters coupled to such resonant nanophotonic structures perceive a modified spatial distribution of emitters. Thus, the spatial extent, strength, and confinement of electromagnetic fields, the hierarchy of distances (and thus the DDI strength) averaging over all possible sites of the interacting emitters is modified. This leads to a modification in the temporal decay dynamics which is reflected in the non-integer exponent, β, and hence, the apparent dimensionality of the interacting system.

System– In this study, we consider the interaction of an ensemble of donor (Alq_3) and acceptor (R6G) emitters in both resonant and off-resonant nanophotonic structures. The dipole-dipole interactions (DDIs) between the emitters lead to resonance energy transfer. The DDI potential is related to the dyadic Green's function, $V_{dd}(\mathbf{r_A}, \mathbf{r_D}; \omega_D) = -(\omega_D^2/\epsilon_0 c^2)\mathbf{n_A}.\overline{\overline{\mathbf{G}}}(\mathbf{r_A}, \mathbf{r_D}; \omega_D).\mathbf{n_D}$, where $\mathbf{r_A}$ and $\mathbf{r_D}$ are the positions of the acceptor and donor emitters, respectively, $\mathbf{n_A}$ and $\mathbf{n_D}$ are unit orientation vectors of the acceptor and donor emitters, respectively, ω_D is the radial frequency of the donor emitter, ϵ_0 is vacuum permittivity, and c is the speed of light [12, 27]. The interaction strength is proportional to the rate of energy transfer, $\Gamma_{ET}(\mathbf{r_A}, \mathbf{r_D}; \omega_D) = (2\pi/\hbar^2)|V_{dd}(\mathbf{r_A}, \mathbf{r_D}; \omega_D)|^2 f_D(\omega_D)\sigma_A(\omega_D)$, where $f_D(\omega_D)$ and $\sigma_A(\omega_D)$ are the emission spectra of the donor emitter and absorption cross-section of the acceptor emitter, respectively. Figure 2(a) shows the spectral overlap between the donor emission spectrum (Alq3), the acceptor absorption spectrum (R6G), and the extinction spectrum of both a resonant and an off-resonant plasmonic lattice. The resonant plasmonic lattice modes mediate the DDIs between the donor and acceptor emitters. The resonant plasmonic lattice modifies the scaling, strength, and range of the DDI potential $|V_{dd}|$ as shown in Fig 2(b). The scaling of the DDI potential, $|V_{dd}|$, is significantly modified with distance $R = |\mathbf{r_D} - \mathbf{r_A}|$ in a resonant structure, whereas the DDI potential decays rapidly with distance in an off-resonant plasmonic lattice. The resonances of the plasmonic lattice modes can be tuned by altering the lattice constant.

The relaxation dynamics of the interacting ensemble of donor-acceptor emitters are governed by non-linear coupled rate equations (see supporting information). Here the Monte-Carlo simulation method is employed to esti-

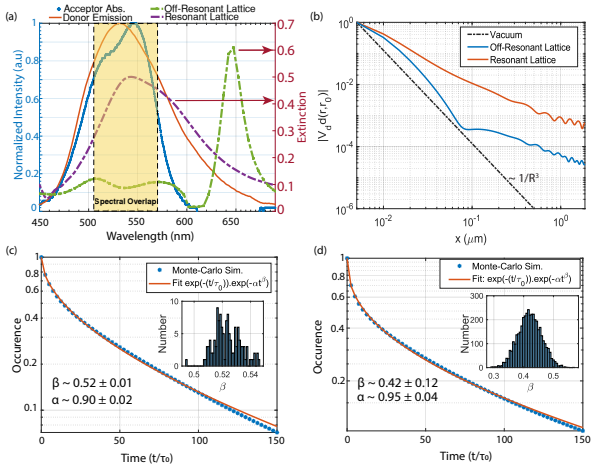

FIG. 2. (a) The plot shows the acceptor emitter's absorption spectrum (blue curve), the donor emitter's emission spectrum (orange curve), the extinction spectrum of a resonant plasmonic lattice with lattice constant $\sim$ 300 nm (purple dash curve) and an off-resonant plasmonic lattice with lattice constant $\sim$ 350 nm (green dash-dot curve). The extinction spectrum of the resonant plasmonic lattice spectrally overlaps with the emission-absorption spectrum of the donor and acceptor emitters (yellow highlighted region) (b) The calculated dipole-dipole interaction potential $|V_{dd}|$ for the resonant and off-resonant plasmonic lattice is shown. The resonant plasmonic lattice shows a strikingly modified scaling law. (c) Monte-Carlo simulations depicting the temporal decay dynamics of donor emitters for $|V_{dd}|^2 = R_0^6/R^6$ scaling and $R_0 \ll L_{sys}$ with $\beta \sim 0.52$. The inset shows the values of β for randomized spatial distributions of emitters. (d) Monte-Carlo simulations showing the temporal decay dynamics of donor emitters for $R_0 \sim L_{sys}$. The reduced dimensionality is evident from the estimated values of $\beta \sim 0.4$. The inset shows the values of β for randomized spatial distributions of emitters.

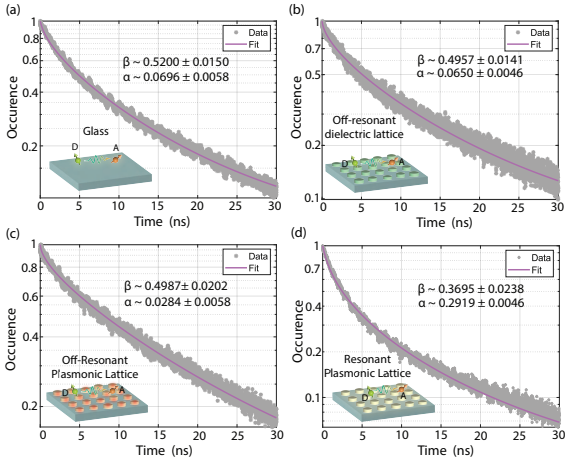

FIG. 3. The measured fluorescence lifetime decay when the interacting emitters are in different electromagnetic environments (a) glass substrate (i.e, a homogeneous environment), (b) TiO2 dielectric lattice (i.e. an off-resonant inhomogeneous electromagnetic environment), and (c) a plasmonic lattice (i.e. a resonant inhomogeneous electromagnetic environment). The value of $\beta \sim 0.5$ in both inhomogeneous and off-resonant inhomogeneous environment. This is commensurate with a 3D system. In contrast, the faster-than-exponential decay dynamics on a resonant silver (Ag) plasmonic lattice reveals an exponent value of ~ 0.37. This is commensurate to an effective lower dimension $\bar{d} \sim 2.20(12)$. The emitters were embedded in a $\sim 1\ \mu m$ thick polymer thin films.

mate the temporal decay dynamics of the donor emitters (see supporting information). Figure 2(c) shows the estimated temporal decay dynamics for homogenous environments, i.e., $R_0 \ll L_{sys}$, where non-integer exponent, $\beta \sim 0.52$. This is commensurate to a three-dimensional interacting system and matches well with the predicted theoretical value (see derivation in supporting information). The inset shows the estimated values of β for various runs of the Monte-Carlo simulations with different random spatial distributions of the emitters. On the other hand when $R_0 \sim L_{sys}$ as shown in Fig.2(d), the value of non-integer exponent, $\beta \sim 0.42(12)$. This is commensurate to an effective dimension of $\bar{d} \sim 2.50(72)$— a lower than a three-dimensional system. The inset shows the broad distribution in the values of β with a standard deviation of ~ 0.12 for 1024 different iterations of the Monte-Carlo simulation.

In practice, a resonant plasmonic lattice aides in realizing an apparent lower-dimensional system. The modified scaling of the DDI potential, $|V_{dd}|$ coupled with increased interaction strength, leads to an increase in the characteristic interaction length scale, R_0. Under certain conditions when the system size, i.e., the spatial extent of emitters, L_{sys} becomes comparable to the R_0 in addition to the scaling law, the interacting system of emitters (in resonant nanophotonic structures) perceive an apparent lower dimension. We explore this effect here to engineer the dimensionality of collective (many-dipole) DDIs.

Experiment– To elucidate this, in the experiment, we measure the fluorescence lifetime decay trace of the interacting emitters in both resonant and off-resonant nanophotonic structures. The dye molecules Alq_3 (0.83 mM) and $R6G$ (0.25 mM) are embedded in PMMA polymer thin films on the aforementioned samples. We use time-correlated single-photon counting technique with a narrow-band filter (520(5) nm) centered at the peak emission of the donor emitter to measure the fluorescence lifetime decay traces (see supporting information for details). Figure 3 shows the measured lifetime decay when the interacting emitters embedded in different nanophotonic structures such as (i) glass substrate, (i.e. a homogeneous environment), Fig.3(a), (ii) a TiO_2 dielectric lattice, Fig.3(b), (iii) an off-resonant plasmonic lattice, Fig.3(c), and (iv) a resonant plasmonic lattice, Fig.3(d). We observe a striking deviation to the non-integer exponent in time from the typical $\beta = 0.5$ in 3D homogeneous environments to $\beta \sim 0.37$ (an effective lower dimension $\bar{d} \sim 2.20(12)$) in a dispersive resonant nanophotonic structure— a plasmonic lattice. We note that this

value is close to that of a 2D system. This elucidates that the underlying resonant modes supported by the plasmonic lattice indeed modify the apparent dimension perceived by the interacting ensemble of emitters. The TiO_2 dielectric lattice has the same geometric features as the resonant plasmonic lattice but supports no resonances. The measurements on the TiO_2 lattice help rule out effects due to the underlying geometry of the lattice. On the other hand, the measurements on the off-resonant plasmonic lattice elucidate that the origin of the apparent lower dimension is purely due to the lattice resonance and not from the localized-surface-plasmon-resonance of the constituent metal nanoparticles.

The non-integer exponent in time is estimated by fitting the temporal fluorescence decay trace with a Laplace transform of an underlying probability density function[26],

$$\frac{I(t)}{I_0} = \int_0^\infty G_\delta(\gamma) e^{-\gamma t} d\gamma \int_0^\infty H_\beta(\Gamma_{ET}) e^{-\Gamma_{ET} t} d\Gamma_{ET} \tag{3}$$

In Eq.3, the first term is associated with the spontaneous decay of donor emitters, whilst the second term is associated with resonance energy transfer (DDIs). $G_\delta(\gamma)$ is the probability density function (PDF) associated with the distribution of spontaneous emission decay rates, and $H_\beta(\Gamma_{ET})$ is the PDF for resonant energy transfer rates. For a homogenous environment, with no significant enhancement in the local density of optical states (LDOS), $G_\delta(\gamma) = \delta(\gamma - \gamma_D)$, where $\delta(\gamma - \gamma_D)$ is the delta function, γ_D is the decay rate of the individual donor emitter. In contrast, in an inhomogeneous environment, each donor experiences different LDOS and, thus, different spontaneous emission decay rates [29]. As DDIs in this particular scenario is a weak perturbation, the spontaneous decay rate of the donors, is estimated from the fluorescence decay trace of donors in the absence of the acceptor emitter(see supporting information). The PDF of resonance energy transfer rates, $H_\beta(\Gamma_{ET})$, is estimated by fitting the fluorescence lifetime decay trace with the spontaneous decay rate PDF, $G_\delta(\gamma)$ as a fixed parameter. The underlying probability distributions have a characteristic long-tail behavior and are related to Lévy stable distributions [30].

Figure 4 shows the extracted PDF of the resonant energy transfer rate (Γ_{ET}) distribution. The PDFs obtained in the resonant inhomogeneous environment are observed to differ from those in the homogeneous and off-resonant inhomogeneous environments. This directly indicates that the sensed spatial distribution of emitters is modified. As the plasmonic lattice supports dispersive delocalized resonant modes that can mediate interactions between the donor and acceptor emitters over larger distances, the underlying PDFs show a broader distribution of rates. Furthermore, the number of interaction events in the tail of the distribution reduces, which indicates a reduction in the total number of larger magnitude DDI interaction strengths, Γ_{ET}, see inset of Fig. 4.

Conclusion- In summary, we experimentally demonstrated that the apparent dimensionality of an interacting ensemble of emitters could be modified using a resonant nanophotonic structure. The temporal fluorescence decay dynamics show a non-integer exponent, β, that relates to the apparent dimensionality of the interacting system. The value of apparent dimensionality on a resonant plasmonic lattice shows a stark contrast value of $\bar{d} \sim 2.20(12)$, in comparison to $\bar{d} \sim 3.0$ obtained on glass, an off-resonant TiO_2 dielectric lattice, and an off-resonant plasmonic lattice. Further, we extract the underlying distribution of energy transfer rates for the emitters' interacting ensemble, indicating that the interacting emitters' perceived apparent dimensionality is modified. This arises due to modifying the underlying distribution of energy transfer rates. This work paves the way for engineering interacting systems with apparent lower dimensionality. Though the presented results are semi-classical and discernible coherent effects cannot be observed at room temperatures, they can readily be applied to regimes where quantum effects are more prominent such as in ultra-cold atoms [14], solid-state emitters systems [1, 2], rare-earth ions [31, 32], Rydberg excitons in solids [33], and quantum-dots systems [13]. Such nanophotonic structures can potentially provide an alternative route to realize two-dimensional systems that host new quantum many-body phases, help mitigate decoherence for quantum sensing, memories, and quantum network applications, realize novel, more efficient light-harvesting systems, and potentially improve biological samples imaging.

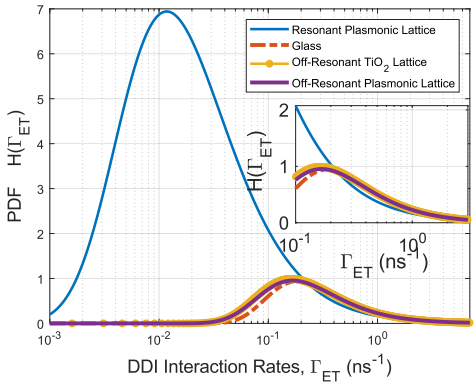

FIG. 4. The extracted probability density function (PDF) for the resonance energy transfer rate on various electromagnetic environments (1) Glass, a homogeneous environment (dash-dot red curve), (2) An in-homogeneous environment, TiO_2 nanoparticle lattice having the same lattice constant and dimensions as the resonant plasmonic lattice (dot-line yellow curve). (3) An off-resonant plasmonic lattice (purple curve) and (4) A resonant plasmonic lattice (blue curve). The PDF of the energy transfer rates on the resonant plasmonic lattice is not only shifted but also broader. The inset shows the reduced number of events having stringer interaction strength (in the tail)

This work was supported by the U.S. Department

of Energy (DOE), Office of Basic Sciences under DE-SC0017717 (A.K.B, A.B, V.S, and Z.J), the Purdue University start-up grant (H.A), the Office of Naval Research (ONR) under ONR N00014-21-1-2289 (Y.W., and T.W.O.) and the National Science Foundation under DMR-2207215 and DMR-1904385 (X.G.J. and T.W.O.). This work made use of the NUFAB and EPIC facilities of Northwestern University's NUANCE Center, which has received support from the SHyNE Resource (NSF ECCS-2025633), the IIN, and Northwestern's MRSEC program (NSF DMR-1720139).

[1] E. J. Davis, B. Ye, F. Machado, S. A. Meynell, W. Wu, T. Mittiga, W. Schenken, M. Joos, B. Kobrin, Y. Lyu, Z. Wang, D. Bluvstein, S. Choi, C. Zu, A. C. B. Jayich, and N. Y. Yao, Probing many-body dynamics in a two-dimensional dipolar spin ensemble, Nature Physics 10.1038/s41567-023-01944-5 (2023).

[2] B. L. Dwyer, L. V. Rodgers, E. K. Urbach, D. Bluvstein, S. Sangtawesin, H. Zhou, Y. Nassab, M. Fitzpatrick, Z. Yuan, K. De Greve, *et al.*, Probing spin dynamics on diamond surfaces using a single quantum sensor, PRX Quantum **3**, 040328 (2022).

[3] C. Broholm, R. Cava, S. Kivelson, D. Nocera, M. Norman, and T. Senthil, Quantum spin liquids, Science **367**, eaay0668 (2020).

[4] N. Y. Yao, M. P. Zaletel, D. M. Stamper-Kurn, and A. Vishwanath, A quantum dipolar spin liquid, Nature Physics **14**, 405 (2018).

[5] L. Chomaz, D. Petter, P. Ilzhöfer, G. Natale, A. Trautmann, C. Politi, G. Durastante, R. Van Bijnen, A. Patscheider, M. Sohmen, *et al.*, Long-lived and transient supersolid behaviors in dipolar quantum gases, Physical Review X **9**, 021012 (2019).

[6] E. Sierra, S. J. Masson, and A. Asenjo-Garcia, Dicke superradiance in ordered lattices: dimensionality matters, Physical Review Research **4**, 023207 (2022).

[7] B. Wittmann, F. A. Wenzel, S. Wiesneth, A. T. Haedler, M. Drechsler, K. Kreger, J. Köhler, E. W. Meijer, H.-W. Schmidt, and R. Hildner, Enhancing long-range energy transport in supramolecular architectures by tailoring coherence properties, Journal of the American Chemical Society **142**, 8323 (2020).

[8] R. Samajdar, W. W. Ho, H. Pichler, M. D. Lukin, and S. Sachdev, Complex density wave orders and quantum phase transitions in a model of square-lattice rydberg atom arrays, Physical Review Letters **124**, 103601 (2020).

[9] M. Schmitt, M. M. Rams, J. Dziarmaga, M. Heyl, and W. H. Zurek, Quantum phase transition dynamics in the two-dimensional transverse-field ising model, Science Advances **8**, eabl6850 (2022).

[10] D. Chang, J. Douglas, A. González-Tudela, C.-L. Hung, and H. Kimble, Colloquium: Quantum matter built from nanoscopic lattices of atoms and photons, Reviews of Modern Physics **90**, 031002 (2018).

[11] W. D. Newman, C. L. Cortes, A. Afshar, K. Cadien, A. Meldrum, R. Fedosejevs, and Z. Jacob, Observation of long-range dipole-dipole interactions in hyperbolic metamaterials, Science advances **4**, eaar5278 (2018).

[12] A. K. Boddeti, J. Guan, T. Sentz, X. Juarez, W. Newman, C. Cortes, T. W. Odom, and Z. Jacob, Long-range dipole–dipole interactions in a plasmonic lattice, Nano letters **22**, 22 (2021).

[13] A. Tiranov, V. Angelopoulou, C. J. van Diepen, B. Schrinski, O. A. D. Sandberg, Y. Wang, L. Midolo, S. Scholz, A. D. Wieck, A. Ludwig, *et al.*, Collective super-and subradiant dynamics between distant optical quantum emitters, Science **379**, 389 (2023).

[14] A. Skljarow, H. Kübler, C. S. Adams, T. Pfau, R. Löw, and H. Alaeian, Purcell-enhanced dipolar interactions in nanostructures, Physical Review Research **4**, 023073 (2022).

[15] A. Goban, C.-L. Hung, J. Hood, S.-P. Yu, J. Muniz, O. Painter, and H. Kimble, Superradiance for atoms trapped along a photonic crystal waveguide, Physical review letters **115**, 063601 (2015).

[16] J. D. Hood, A. Goban, A. Asenjo-Garcia, M. Lu, S.-P. Yu, D. E. Chang, and H. Kimble, Atom–atom interactions around the band edge of a photonic crystal waveguide, Proceedings of the National Academy of Sciences **113**, 10507 (2016).

[17] T. Förster, Experimentelle und theoretische untersuchung des zwischenmolekularen übergangs von elektronenanregungsenergie, Zeitschrift für naturforschung A **4**, 321 (1949).

[18] J. Drake, J. Klafter, and P. Levitz, Chemical and biological microstructures as probed by dynamic processes, Science **251**, 1574 (1991).

[19] L. Klushin and O. Tcherkasskaya, Effects of molecular distribution on the fluorescence transfer: Exact results for slab geometry, The Journal of chemical physics **119**, 3421 (2003).

[20] B. Neyenhuis, J. Zhang, P. W. Hess, J. Smith, A. C. Lee, P. Richerme, Z.-X. Gong, A. V. Gorshkov, and C. Monroe, Observation of prethermalization in long-range interacting spin chains, Science advances **3**, e1700672 (2017).

[21] D. A. Abanin, E. Altman, I. Bloch, and M. Serbyn, Colloquium: Many-body localization, thermalization, and entanglement, Reviews of Modern Physics **91**, 021001 (2019).

[22] L. Ratschbacher, C. Sias, L. Carcagni, J. Silver, C. Zipkes, and M. Köhl, Decoherence of a single-ion qubit immersed in a spin-polarized atomic bath, Physical review letters **110**, 160402 (2013).

[23] H. Takano, H. Nakanishi, and S. Miyashita, Stretched exponential decay of the spin-correlation function in the kinetic ising model below the critical temperature, Physical Review B **37**, 3716 (1988).

[24] G. Kucsko, S. Choi, J. Choi, P. C. Maurer, H. Zhou, R. Landig, H. Sumiya, S. Onoda, J. Isoya, F. Jelezko, *et al.*, Critical thermalization of a disordered dipolar spin system in diamond, Physical review letters **121**, 023601 (2018).

[25] R. Hanson, V. Dobrovitski, A. Feiguin, O. Gywat, and D. Awschalom, Coherent dynamics of a single spin interacting with an adjustable spin bath, Science **320**, 352 (2008).

[26] M. Berberan-Santos, E. Bodunov, and B. Valeur, Mathematical functions for the analysis of luminescence decays with underlying distributions 1. kohlrausch decay function (stretched exponential), Chemical Physics **315**, 171 (2005).

[27] C. L. Cortes and Z. Jacob, Super-coulombic atom–atom interactions in hyperbolic media, Nature communications **8**, 14144 (2017).

[28] S.-A. Biehs, V. M. Menon, and G. Agarwal, Long-range dipole-dipole interaction and anomalous förster energy transfer across a hyperbolic metamaterial, Physical Review B **93**, 245439 (2016).

[29] G. M. Akselrod, C. Argyropoulos, T. B. Hoang, C. Ciracì, C. Fang, J. Huang, D. R. Smith, and M. H. Mikkelsen, Probing the mechanisms of large purcell enhancement in plasmonic nanoantennas, Nature Photonics **8**, 835 (2014).

[30] H. K. Nakamura, M. Sasai, and M. Takano, Scrutinizing the squeezed exponential kinetics observed in the folding simulation of an off-lattice go-like protein model, Chemical physics **307**, 259 (2004).

[31] A. Ruskuc, C.-J. Wu, J. Rochman, J. Choi, and A. Faraon, Nuclear spin-wave quantum register for a solid-state qubit, Nature **602**, 408 (2022).

[32] M. T. Uysal, M. Raha, S. Chen, C. M. Phenicie, S. Ourari, M. Wang, C. G. Van de Walle, V. V. Dobrovitski, and J. D. Thompson, Coherent control of a nuclear spin via interactions with a rare-earth ion in the solid state, PRX Quantum **4**, 010323 (2023).

[33] T. Kazimierczuk, D. Fröhlich, S. Scheel, H. Stolz, and M. Bayer, Giant rydberg excitons in the copper oxide cu2o, Nature **514**, 343 (2014).